ELSEVIER

Mixed pyrazolylborate/cyclopentadienyl derivatives of divalent lanthanides: synthesis and structure of $(Tp^{'Bu,Me})Yb(C_5H_4R)$ (R = H, SiMe$_3$)

Gregory M. Ferrence [1], Robert McDonald, Martin Morissette [2], Josef Takats *

Department of Chemistry, University of Alberta, Edmonton, AB, Canada T6G 2G2

Dedicated to Professor F.A. Cotton on the occasion of his 70th birthday.

Abstract

Reaction of $[(Tp^{'Bu,Me})YbH]_2$ with cyclopentadiene (C_5H_6) and trimethylsilyl cyclopentadiene ($C_5H_5SiMe_3$) resulted in the formation of the corresponding mixed-ligand complexes, $(Tp^{'Bu,Me})Yb(C_5H_4R)$ (R = H, **1a**; SiMe$_3$, **1b**), in an essentially quantitative yield. The complexes were characterized by multinuclear NMR spectroscopy and, **1b**, by single-crystal X-ray diffraction. The solid-state structure of **1b** consists of well-separated monomeric units with a η^5-C$_5$H$_4$SiMe$_3$ ring, but the Tp$^{'Bu,Me}$ ligand exhibits an unusual distortion; one of the pyrazolyl rings is rotated in such a way as to bring both pyrazolyl nitrogens in bonding contact with ytterbium. The simple ^{1}H- and ^{13}C-NMR spectra of one set of Tp$^{'Bu,Me}$ resonances indicate fluxional solution behavior. The barrier to pyrazolyl ring exchange is very small since no line broadening was observed down to −100°C. © 2000 Elsevier Science S.A. All rights reserved.

1. Introduction

The rapid and spectacular development of the organometallic chemistry of divalent lanthanides (Ln(II) = Sm, Eu, Yb) is largely due to the introduction of the pentamethyl–cyclopentadienyl ligand to this area of chemistry [1]. Following the early successes, it was natural to explore the ability of other ancillary ligands to stabilize 'LnL$_2$'-type species. In view of the importance of steric factors in lanthanide chemistry, it is not surprising that a prerequisite is the use of bulky ligands and, by now, a good variety of such ligands have been investigated [2]; recent examples include bulky pyrazolate [3] and hydrotris(pyrazolyl)borate [4] derivatives.

However, despite the now well-established homoleptic 'LnL$_2$' complexes, heteroleptic divalent lanthanide compounds are rare; recent examples are some mixed C$_5$Me$_5$/ER (ER = OAr, SAr, NR^{1}R^2) Sm(II) complexes which also exhibit remarkable reactivities [5]. In this context, we have shown that the very bulky hydrotris(3-*tert*-butyl-5-methylpyrazolyl)borate (Tp$^{'Bu,Me}$) ligand is well suited to stabilize the mono-ligated complexes (Tp$^{'Bu,Me}$)LnI(THF)$_x$ (Ln = Yb, $x = 1$; Sm, $x = 2$, 0), which proved to be versatile starting materials for the synthesis of heteroleptic (Tp$^{'Bu,Me}$)LnER (Ln = Sm, Yb; ER = N(SiMe$_2$)$_2$, CH(SiMe$_3$)$_2$; Ln = Yb; ER = OAr, CH$_2$SiMe$_3$) compounds [6], culminating in the isolation of the first discrete Ln(II) hydride, $[(Tp^{'Bu,Me})YbH]_2$ [7]. Here we report that the latter compound allows the preparation of ytterbium(II) compounds containing both pyrazolylborate and cyclopentadienyl groups.

* Corresponding author. Tel.: +1-780-492-4944; fax: +1-780-492-8231.

E-mail address: joe.takats@ualberta.ca (J. Takats).

[1] Present address: Department of Chemistry, Illinois State University, Normal, IL 61761-4160, USA.

[2] Summer undergraduate research student.

2. Results and discussion

With the availability of $[(Tp^{'Bu,Me})YbH]_2$ and its demonstrated facile reaction toward protic substances [7], it was of interest to investigate whether the compound will also be a useful starting material for mixed ytterbium(II) pyrazolylborate–cyclopentadienyl complexes. Protonolysis offers an alternative, and often more convenient and trouble-free, synthetic route to lanthanide complexes than classical salt-metathesis. In particular, the possibility of using non-coordinating hydrocarbon or aromatic solvents allows the isolation of unsolvated compounds, a highly desirable but normally difficult task with the strongly Lewis acidic lan-
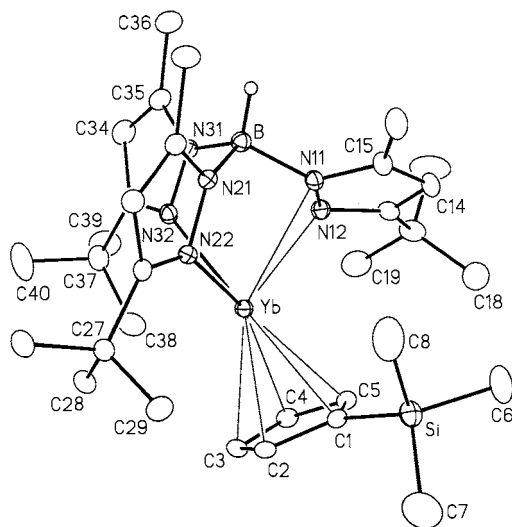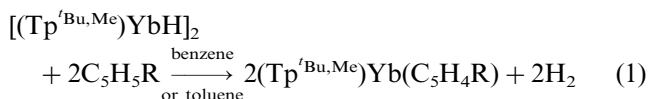
thanide ions.

Reaction of the Yb(II)-hydride with stoichiometric amounts of cyclopentadiene or trimethylsilyl cyclopentadiene proceeded readily and gave, after simple work-up, the corresponding heteroleptic complexes **1a** and **1b** in almost quantitative yields (Eq. (1)):

$$[(Tp^{'Bu,Me})YbH]_2$$
$$+ 2C_5H_5R \xrightarrow[\text{or toluene}]{\text{benzene}} 2(Tp^{'Bu,Me})Yb(C_5H_4R) + 2H_2 \quad (1)$$

R = H, **1a** (orange), R = SiMe₃, **1b** (red–orange)

As noted previously by Lappert et al. [8], the presence of the SiMe₃ group results in greater solubility and, more importantly, better crystallinity of **1b** than **1a**. The complexes are highly air sensitive and moderately stable in the solid state. They can be crystallized from toluene, but an attempt to crystallize **1a** from pentane led to decomposition and formation of $Yb(Tp^{'Bu,Me})_2$ [9] as a result of ligand redistribution. A mixture of products was also obtained from the reaction of the hydride with indene, $Yb(Tp^{'Bu,Me})_2$ being a major component, whereas pentamethylcyclopentadiene (C_5Me_5H) failed to react.

The formulation of the complexes is based on elemental analyses, IR and multinuclear (^1H-, ^{13}C-, ^{11}B- and ^{171}Yb-) NMR spectroscopies. The ^1H- and ^{13}C-NMR spectra of both **1a** and **1b** showed one set of signals for the $Tp^{'Bu,Me}$ ligand; the position of the B–H signal was obtained from a $^1H\{^{11}B\}$-NMR spectrum. The ^1H-NMR spectra also showed resonances due to protons of the cyclopentadienyl ligands. In **1a** this was a sharp singlet at 6.67 ppm, whereas in **1b** three resonances were observed at 0.26 ppm (SiMe₃), and two multiplets, each integrating as 2H, at 6.68 and 6.86 ppm, respectively. Single peaks were also observed in the $^{11}B\{^1H\}$- and $^{171}Yb\{^1H\}$-NMR spectra. Interestingly, the ^{171}Yb chemical shift of **1b** (201 ppm) is 100 ppm downfield of that in **1a** (101 ppm). A similar downfield shift upon SiMe₃ substitution in cyclopentadienyl ligands was noted by Lappert and co-workers in ytterbocene(II) complexes containing pendant pyridyl groups [8b].

Although consistent with the molecular formulation, the simple spectroscopic signatures left open the question whether this was due to symmetrical bonding between the Yb(II) center and the $Tp^{'Bu,Me}/C_5H_4R$ ligands or to asymmetric bonding and solution fluxional behavior. To resolve this ambiguity the solid-state structure of **1b** was determined by a single-crystal X-ray diffraction study.

The molecular structure and atom numbering scheme for crystalline $(Tp^{'Bu,Me})Yb(C_5H_4SiMe_3)$ (**1b**) are shown in Fig. 1; selected bond lengths and angles are listed in Table 1. The Yb(II) center is bonded to a η^5-$C_5H_4SiMe_3$ ring but its interaction with the $Tp^{'Bu,Me}$ ligand is far from symmetrical. While two of the pyr-

Fig. 1. Perspective view of $(Tp^{'Bu,Me})Yb(C_5H_4SiMe_3)$ (**1b**) showing the atom labeling scheme. Non-hydrogen atoms are represented by Gaussian ellipsoids at the 20% probability level; hydrogen atom attached to boron is shown with an arbitrarily small thermal parameter, all other hydrogens are not shown.

Table 1
Selected bond lengths (Å) and bond angles (°) for **1b**

Bond lengths

Yb–N11	2.748(3)	Yb–C1	2.762(3)
Yb–N12	2.512(3)	Yb–C2	2.744(3)
Yb–N22	2.497(3)	Yb–C3	2.715(3)
Yb–N32	2.443(3)	Yb–C4	2.689(3)
B–N11	1.579(5)	Yb–C5	2.706(3)
B–N21	1.550(5)	C1–C2	1.426(4)
B–N31	1.534(5)	C2–C3	1.397(5)
N11–N12	1.395(4)	C3–C4	1.412(5)
N21–N22	1.375(4)	C4–C5	1.395(5)
N31–N32	1.366(5)	C5–C1	1.418(5)

Bond angles

Yb–N11–N12	65.5(2)	N11–Yb–N12	30.4(8)
Yb–N12–N11	84.2(2)	N11–Yb–N22	72.4(8)
Yb–N22–N21	109.6(2)	N11–Yb–N32	72.4(9)
Yb–N32–N31	110.7(2)	N12–Yb–N22	101.6(9)
N22–Yb–N32	74.2(9)	N12–Yb–N32	72.5(9)

Table 2
Selected structural data on some Yb(II)–cyclopentadienyl complexes

Complex	CN [a]	Average Yb–C (Å)	EIR Cp′ (Å) [b]	Cp′–Yb–Cp′ (°) [c]	Ref.
$Yb(C_5H_5)_2(DME)$	8	2.658	1.52	133.9	[14]
$Yb(C_5H_4SiMe_3)_2(THF)_2$	8	2.75	1.61	133	[8a]
$Yb(C_5Me_5)_2(py)_2$	8	2.74(4)	1.60	136.3(3)	[15]
$Yb(C_5Me_5)_2(THF)$	7	2.663	1.58	143.5(3)	[16]
$[Yb\{C_5H_3(SiMe_3)_2\}_2]_\infty$	7	2.662	1.58	138	[17]
$Yb(C_5Me_5)_2$	6	2.665(4)	1.64	145.5 [d]	[18]
$(Tp'^{Bu,Me})Yb(C_5H_4SiMe_3)$	7	2.723	1.64	154.6 [e]	This work

[a] Coordination number.

[b] Effective ionic radius of the cyclopentadienyl ring; obtained by subtracting from the average Yb–C distance the effective ionic radius of Yb^{2+} (1.14 Å for CN 8, 1.08 Å for CN 7, 1.02 Å for CN 6 [19]).

[c] Cp′ ring centroid–Yb–Cp′ ring centroid angle.

[d] Average of the two independent molecules in the unit cell.

[e] This is the B–Yb–Cp′ ring centroid angle.

azolyl moieties interact the usual way (lone-pair dona- tion from 2-N), the third pyrazolyl ring is rotated such as to bring both nitrogens, N12 and N11, into contact with ytterbium. This is evidenced by the large Yb–N12–N11–B torsional angle, 75.3(3)°, compared with 14.9(3) and 14.3(3)° for the other two pyrazolyl rings. The Yb–N12/N22/N32 distances (2.512(3), 2.497(3) and 2.443(3) Å, respectively) are similar to those found in $Yb(Tp^{Me_2})_2$ (2.482(5) Å) and $Yb(Tp^{Ph})_2$ (2.55(2) Å) [4b,6c]. Although the Yb–N11 contact, 2.748(3) Å, is 0.2 Å longer than Yb–N12, it is clearly within bonding distance. Further evidence of the side- on interaction with both N12 and N11 comes from comparison of the respective B–N and N–N distances. Although at the threshold of being significant, the trends are clear. As expected from coordination, both distances are slightly longer in the rotated pyrazolyl ring. As a final corroborating point, we note that the Yb⋯B separation of 3.196(4) Å is much shorter than the ca. 3.5 Å in $Yb(Tp^{Me_2})_2$ and $Yb(Tp^{Ph})_2$ complexes that contain two symmetrical, tridentate $Tp^{R,R'}$ ligands. Similar distortions of the $Tp^{R,R'}$ ligands have been observed before in $U(Tp^{Me_2})_2I$ [10], $Sm(Tp^{Me_2})_2(SePh-4-'Bu)$ and $Sm(Tp^{Me_2})_2(SePh)$ [11], and the corresponding torsional angles and M–N distances are; U(III) complex 87.4°, 2.833(5) and 2.807(5) Å; Sm(III) complexes 91.3°, 2.736(2) and 2.858(2) Å, and 83.7°, 2.819(2) and 2.740(2) Å. Interestingly, rotation of one of the pyra- zolyl rings is also seen in the recently reported structure of $(PhTp'^{Bu})Tl$ where the twist angle is ca. 90° [12]. However, in this case the Tl only interacts with the nitrogen atom attached directly to boron, the unique Tl–N(pz) distance, 2.833(2) Å, is significantly longer than the two conventional Tl–N(pz) bonds (2.528(3) and 2.585(3) Å). Thus, contrary to the f-element com- plexes, where rotation of the pyrazolyl ring is accompa- nied by an increase in the number of M–N(pz) interactions, the denticity of the $PhTp'^{Bu}$ ligand in the Tl complex remains the same at three. With a decrease

in Tl–N(pz) bonding, the main reason for the twisting is thought to be relief of steric interactions between the phenyl group at boron and the pyrazolyl 5-H sub- stituents. Support for the steric argument comes from the structure of a series of $(Tp^{R,R'})Tl$ complexes which lack the phenyl substituent at boron [13]. The structure of all complexes, including those of $(Tp'^{Bu,Me})Tl$ and $(Tp'^{Bu_2})Tl$, exhibit symmetrical tridentate $Tp^{R,R'}$ ligands bonded to Tl via 2-N of the pyrazolyl rings. With no bulky substituent at boron, and hence the absence of intraligand steric repulsion in the f-element complexes, electronic factors must play a role in the observed side-on bonded $(\eta^2\text{-pz})$–M geometry. Unfortunately the range of M–N distances and twist angles precludes a ranking of the strength of the interaction, except to say that distortion of the $Tp^{R,R'}$ ligand appears to be facile in these complexes where the bonding between the f-metal ion and the ligand is mainly ionic in nature.

Returning to the $Yb\text{-}(\eta^5\text{-}C_5H_4SiMe_3)$ portion of the molecule, the Yb–C distances range from 2.689(3) to 2.762(3) Å, with an average of 2.72 Å and Yb–Cp′ (Cp′ is the centroid of the ring) distance of 2.45 Å. A summary of some relevant structural data in related Yb(II)–cyclopentadienyl complexes is given in Table 2. Both the average Yb–C distance, at the upper end of the range, and the effective ionic radius of the $C_5H_4SiMe_3$ ring, comparable with that of C_5Me_5 lig- and, are indicative of the sterically congested nature of the ytterbium center in **1b**; the bulky $Tp'^{Bu,Me}$ ligand prevents closer approach of the $C_5H_4SiMe_3$ ring. We believe that steric factors are also responsible for the nonlinearity of the B–Yb–Cp′ vector. Reference to Fig. 1 shows that movement of the $C_5H_4SiMe_3$ group away from linearity is to reduce repulsion between the ring and 'Bu groups at C27 and C37; the closest contacts are C28⋯C2 3.67 and C38⋯C3 3.66 Å. The rotational orientation of the cyclopentadienyl ring is such as to position the $SiMe_3$ moiety in the space created by the pyrazolyl group N21/N22 and the twisted pyrazolyl

ring. There is no extra stabilization gained from agostic interaction since the Yb⋯C8 separation (4.17 Å) is longer than the sum of the van der Waals radii (3.8 Å). The Yb⋯C38 (3.24 Å) distance is at the upper end of the range where intramolecular agostic interactions in organoytterbium complexes are thought to occur, however the absence of deviation from tetrahedral geometry of the ^{t}Bu group, C37, indicates that such interactions are of no importance in the present case. The Yb⋯C28 distance is 3.70 Å.

It is instructive to compare the molecular structure of **1b** with those of other Yb(II) complexes containing the Tp$^{^tBu,Me}$ ligand. In the series of (Tp$^{^tBu,Me}$)YbER complexes (ER = N(SiMe$_3$)$_2$ [6a], CH(SiMe$_3$)$_2$ [6a], OC$_6$H$_2$-Me$_3$ [20]), and even in those containing another ligand, (Tp$^{^tBu,Me}$)YbI(THF) [6a] and (Tp$^{^tBu,Me}$)Yb(OC$_6$H$_2$Me$_3$)-(THF) [20] or the bidentate pyvalate, (Tp$^{^tBu,Me}$)Yb-(pivalate) [20], the Tp$^{^tBu,Me}$ ligand adopts its usual tridentate bonding mode and coordinates to Yb via the lone pair of the pyrazolyl rings 2-N donor atom. Interaction with the other ligand(s) is also via σ-lone-pair donation. The rotational flexibility offered by such bonding is apparently sufficient to allow the substituents of the ligand(s) to fit between the end-on bonded pyrazolyl rings and to maintain the common trigonal (C$_3$) η^3-coordination of the Tp$^{^tBu,Me}$ ligand. In the present case, such bonding mode of the sterically demanding Tp$^{^tBu,Me}$ ligand would necessitate an η^1-C$_5$H$_4$SiMe$_3$ moiety, akin to the CH(SiMe$_3$)$_2$ ligand. This would be a rather unusual situation since, in the lanthanide realm, monohapto-cyclopentadienyl group has so far been encountered only when it bridges two lanthanide ions [21], the overwhelming preponderance is for the η^5-cyclopentadienyl bonding mode [1,22]. This is what happens in **1b** and indeed the situation is the same in the recently prepared and structurally characterized Sm(III) mixed Tp/Cp complexes, Sm(η^3-Tp^{Me_2})(η^2-Tp^{Me_2})(η^5-C$_5$H$_5$) [23] and Sm(η^5-C$_5$Me$_5$)$_2$-(η^2-Tp^{Me_2}) [24], although the hapticity change induced in the Tp^{Me_2} ligand is different from that seen in **1b**. It is clear from Fig. 1 that distortion of the Tp$^{^tBu,Me}$ ligand from the symmetric η^3-bonding is due to the strong steric repulsion between the η^5-C$_5$H$_4$SiMe$_3$ group and the pyrazolyl ring, exacerbated in the present case by the presence of the ^{t}Bu substituent at the three-position. Complete removal of one of the pyrazolyl groups and formation of an η^2-Tp$^{^tBu,Me}$ ligand, with perhaps additional BH⋯Yb(II) interaction [9], would probably be the most favorable situation from the point of view of relieving non-bonding interactions, but apparently such an outcome would have left the Yb(II) center electron deficient. Rotation of the pyrazolyl ring about the B–N axis also relieves the steric interactions between it and the C$_5$H$_4$SiMe$_3$ ligand, while maintaining the Yb–N(pz) bonding, in particular, the electronic stabilization gained from the additional Yb–N11 interaction must be important as well.

As a result of the extra interaction, due to the side-on η^2-bonded pyrazolyl ring, the formal coordination number of ytterbium is seven. Anything higher than this would necessitate further interaction with the rotated pyrazolyl group. Although coordination modes η^3- and even η^5- for a pyrazolate ligand have been reported, [K{Er(^{t}Bu$_2$pz)$_4$}$_n$] [25] and (C$_5$Me$_5$)-(Me$_2$pz)Ru [26], respectively, the long Yb–C distances in **1b** (Yb-C13 3.49, Yb–C15 3.79 and Yb–C14 4.16 Å) argue against any such consideration.

Attractive intermolecular interactions can be important and are pervasive in lanthanide–cyclopentadienyl complexes. They range from bridging cyclopentadienyl units, of varying hapticity in polymeric structures [1,21] to the weak, agostic γ-methyl–metal interactions identified by Lappert and co-workers in [Yb(η-Cp″)$_2$]$_∞$ and [Eu(η-Cp″)$_2$]$_∞$ (Cp″ = C$_5$H$_3$(SiMe$_3$)-1,3) [17] and may involve aromatic C$_6$H$_6$ moieties [27]. There are no such unusual intermolecular contacts in crystalline **1b**. The solid-state structure consists of well-separated monomeric units, reflecting the large size of the Tp$^{^tBu,Me}$ ligand and the sterically congested nature of **1b**. Although **1b** crystallizes with 0.5 toluene per ytterbium, the closest Yb–C(toluene) distance is 5.96 Å, clearly showing that the toluene functions only as a molecule of crystallization.

The distorted C$_1$ solid-state structure of **1b** is not in accord with its ^{1}H- and ^{13}C-NMR spectra which therefore indicate fluxional behavior in solution. Attempts to slow down the fluxionality were not successful. The ^{1}H-NMR spectrum of **1a** and **1b**, recorded in toluene-d_8, remained invariant down to −100°C except for some viscosity broadening and some temperature-dependent chemical shift of the cyclopentadienyl ring resonances.

3. Experimental

3.1. Materials and procedures

All manipulations were carried out under inert N$_2$–He atmosphere in a Vacuum Atmosphere HE-553-2 Dri Lab. Glassware and solvents were treated as described previously [9]. [(Tp$^{^tBu,Me}$)YbH]$_2$ was prepared according to published procedure [7].

Infrared (IR) spectra were recorded on a Nicolet Magna 750 FT Spectrometer. NMR samples were prepared in a glove box and sealed under vacuum. The spectra were obtained on a Brüker AM-400 or Varian Unity 500 (^{171}Yb) FT spectrometer. Chemical shifts are reported in ppm relative to TMS (^{1}H, ^{13}C), F$_3$B·OEt$_2$ (^{11}B) and Yb(C$_5$Me$_5$)$_2$(THF)$_2$ (^{171}Yb). Elemental analy-

ses were performed by the Microanalytical Laboratory, Department of Chemistry, University of Alberta.

3.2. Synthesis of $(Tp^{'Bu,Me})Yb(C_5H_5)$ (1a)

To a slurry of $[(Tp^{'Bu,Me})YbH]_2$ (414 mg, 0.347 mmol) in 10 ml of benzene was added 47 μl (0.693 mmol) of freshly 'cracked' cyclopentadiene (C_5H_6). The mixture was stirred at room temperature (r.t.) resulting in gradual dissolution of the hydride. After 2 h of stirring the solvent was removed in vacuo to give 446 mg of $(Tp^{'Bu,Me})Yb(C_5H_5)$ (1a) as an orange solid (Yield 97%). Further crystallization did not improve the purity of the product. IR (thin film, C_6H_6, cm^{-1}): ν_{B-H} 2525. ^{1}H-NMR (C_6D_6, 25°C, ppm): 6.67 (C_5H_5), 5.70 (s, 4-H), 4.50 (s, B–H; from ^{1}H{^{11}B}), 1.99 (s, CH_3), 1.43 (s, C(CH_3)$_3$). ^{13}C-NMR, APT (C_6D_6, 25°C, ppm): 13.13 (CH_3), 31.39 (C(CH_3)$_3$), 32.18 (C(CH$_3$)$_3$), 103.7 (4-CH), 111.1 (C_5H_5), 146.4 (3-C), 164.7 (5-C). ^{11}B{^{1}H}-NMR (C_6D_6, 25°C, ppm): -7.7 (s, $\Delta\nu_{1/2} = 150$ Hz). ^{171}Yb-NMR (toluene-d_8, 25°C, ppm): 101 ($\Delta\nu_{1/2} = 50$ Hz) (-80°C; 117 ppm). Anal. Calc. for $C_{29}H_{45}BN_6Yb$: C, 52.65; H, 6.86; N, 12.70. Found: C, 51.55; H, 7.10; N, 12.45.

3.3. Synthesis of $(Tp^{'Bu,Me})Yb(C_5H_4SiMe_3)$ (1b)

To a slurry of $[(Tp^{'Bu,Me})YbH]_2$ (500 mg, 0.419 mmol) in 3 ml of toluene was added 134 mg (0.838 mmol) of trimethylsilylcyclopentadiene ($C_5H_5SiMe_5$). As the mixture was stirred at r.t. the hydride gradually dissolved and the solution became deep red; evolution of H_2 bubbles signaled the reaction between the Yb(II)-hydride and $C_5H_5SiMe_3$. After 2 h of stirring the volume of the solution was reduced in vacuo to ca. 0.5 ml. Cooling at -40°C overnight resulted in the formation of red–orange crystals. The supernatant liquid was decanted from the crystals and the solvent was removed in vacuo, giving more $(Tp^{'Bu,Me})Yb$-($C_5H_4SiMe_3$) (1b) as red–orange solid; combined yield 570 mg (89%, based on 0.3 molecules of toluene of crystallization per ytterbium from the ^{1}H-NMR spectrum).

^{1}H-NMR (C_6D_6, 25°C, ppm): 0.26 (s, Si(CH_3)$_3$), 1.42 (s, C(CH_3)$_3$), 2.00 (s, CH_3), 5.69 (s, 4-H), 4.44 (s, B–H; from ^{1}H{^{11}B}), 6.68 (m, 2H, $C_5H_4SiMe_3$), 6.86 (m, 2H, $C_5H_4SiMe_3$). Additional signals at 2.10(s) and 7.01–7.11(m) from 0.3 molecules of toluene of crystallization per ytterbium. ^{13}C-NMR (C_6D_6, 25°C, ppm): 0.87 (Si(CH_3)$_3$), 12.97 (CH_3), 31.30 (C(CH_3)$_3$), 32.33 (C(CH$_3$)$_3$), 103.76 (4-CH), 112.88 ($C_{2,5}$ of $C_5H_4SiMe_3$), 119.25 ($C_{3,4}$ of $C_5H_4SiMe_3$), 147.14 (3-C), 164.67 (5-C). ^{11}B{^{1}H} (C_6D_6, 25°C, ppm): -6.58 ($\Delta\nu_{1/2} = 170$ Hz), ^{171}Yb-NMR (C_6D_6, 25°C, ppm): 201 ($\Delta\nu_{1/2} = 25$ Hz). Anal. Calc. for $C_{32}H_{53}BN_6SiYb$: C, 52.38; H, 7.28; N,

11.45. Found: C, 52.27; H, 7.14; N, 11.08%. (The calculated values for $C_{32}H_{55}BN_6SiYb \cdot 0.3PhMe$ are C, 53.79; H, 7.33; N, 11.04.)

3.4. Reaction of $[(Tp^{'Bu,Me})YbH]_2$ with C_5Me_5H

To a solution of $[(Tp^{'Bu,Me})YbH]$ in 0.8 ml of C_6D_6 in an NMR tube was added a stoichiometric amount of C_5Me_5H. The ^{1}H-NMR spectrum showed no immediate reaction. Heating the solution to 70°C for 18 h led to decomposition.

3.5. X-ray structure determination of $[(Tp^{'Bu,Me})Yb(C_5H_4SiMe_3)] \cdot 0.5PhMe$ (1b · 0.5PhMe)

Red–orange crystals of $[(Tp^{'Bu,Me})Yb(C_5H_4SiMe_3)] \cdot$ 0.5PhMe (1b · 0.5PhMe) were obtained from cooling a saturated toluene solution of the compound. Data were collected on a Brüker P4/RA/SMART 1000 CCD diffractometer [28] using Mo–K$_\alpha$ radiation at -80°C. Unit cell parameters were obtained from a least-squares refinement of the setting angles of 6741 reflections from the data collection. The systematic absences indicated the space group to be $P2_1/c$ (No. 14). The data were corrected for absorption through use of the SADABS procedure. See Table 3 for a summary of crystal data and X-ray data-collection information.

The structure of 1b·0.5PhMe was solved using the direct methods program SHELXS-86 [29] and refinement was completed using the program SHELXL-93 [30]. Hydrogen atoms were assigned positions based on the geometries of their attached carbon atoms, and were given thermal parameters 20% greater than those of the attached carbons. Restraints were applied to impose an idealized geometry upon the inversion-disordered solvent toluene molecule (see Table 3, footnote c for details. The final model for 1b·0.5PhMe refined to values of $R_1(F) = 0.0262$ (for 6331 data with $F_o^2\varepsilon2\sigma(F_o^2)$) and $wR_2(F^2) = 0.0739$ (for all 7415 independent data).

4. Supplementary material

Tables of final atomic coordinates, thermal parameters, and interatomic distances, angles and torsional angles have been deposited with the Cambridge Crystallographic Data Centre, CCDC no. 134332. Copies of this information may be obtained free of charge from the Director, CCDC, 12 Union Road, Cambridge, CB2 1EZ, UK (Fax: $+44$-1223-336033; e-mail: deposit@ ccdc.ca.ac.uk or www: htp://www.ccdccam.ac.uk).

Table 3
Crystallographic experimental details for **1b**·0.5PhMe

A. *Crystal data*

Empirical formula	$C_{35.5}H_{57}BN_6SiYb$
Formula weight	779.81
Crystal dimensions (mm)	$0.42 \infty 0.40 \infty 0.26$
Crystal system	Monoclinic
Space group	$P2_1/c$ (No. 14)
Unit cell dimensions [a]	
a (Å)	14.3414 (7)
b (Å)	10.4478 (5)
c (Å)	26.2283 (14)
β (°)	96.6020 (10)
V (Å^3)	3903.9 (3)
Z	4
$D_{calc.}$ (g cm^{-3})	1.327
μ (mm^{-1})	2.457

B. *Data-collection and refinement conditions*

Diffractometer	Brüker P4/RA/SMART 1000 CCD
Radiation (λ [Å])	Graphite-monochromated Mo–K$_\alpha$ (0.71073)
Temperature (°C)	-80
Scan type	ϕ rotations (0.3−)/ω scans (0.3−) (20 s exposures)
Data collection 2θ limit (°)	51.50
Total data collected	20 112 ($-17 \leq h \leq 16$, $-12 \leq k \leq 12$, $-31 \leq l \leq 31$)
Independent reflections	7415
Number of observations	6331 [$F_o^2 \varepsilon 2\sigma(F_o^2)$]
Refinement method	Full-matrix least-squares on F^2 (SHELXL–93 [b])
Structure solution method	Direct methods (SHELXS–86)
Absorption correction method	SADABS
Range of transmission factors	0.6239–0.3989
Data/restraints/parameters	7415 [$F_o^2 \varepsilon - 3\sigma(F_o^2)$]/16 [c]/384
Goodness-of-fit (S) [d]	1.060 [$F_o^2 \varepsilon - 3\sigma(F_o^2)$]
Final R indices [e]	
R_1 [$F_o^2 \varepsilon 2\sigma(F_o^2)$]	0.0262
wR_2 [$F_o^2 \varepsilon - 3\sigma(F_o^2)$]	0.0739
Largest difference peak and hole (e Å^{-3})	1.151 and -1.228

[a] Obtained from least-squares refinement of 6741 centered reflections.

[b] Refinement on F_o^2 for all reflections (all of these having $F_o^2 \varepsilon - 3\sigma(F_o^2)$). Weighted R factors wR_2 and all goodness-of-fit S values are based on F_o^2; conventional R factors R_1 are based on F_o, with F_o set to zero for negative F_o^2. The observed criterion of $F_o^2 > 2\sigma(F_o^2)$ is used only for calculating R_1, and is not relevant to the choice of reflections for refinement. R factors based on F_o^2 are statistically about twice as large as those based on F_o, and R factors based on all data will be even larger.

[c] Restraints were applied to impose an idealized geometry upon the inversion-disordered solvent toluene molecule: $d(C90–C91) = d(C91–C92) = d(C91–C92') = d(C92–C93) = d(C93–C90') = d(C90'–C94) = d(C94–C92') = 1.42$ Å; $d(C90 \cdots C92) = d(C90 \cdots C92') = d(C91 \cdots C93) = d(C91 \cdots C94) = d(C92 \cdots C92') = d(C93 \cdots C94) = 2.46$ Å; $d(C91 \cdots C90') = d(C92 \cdots C94) = d(C93 \cdots C92') = 2.84$ Å (primed atoms are related to unprimed ones via the crystallographic inversion center $(0, \frac{1}{2}, \frac{1}{2})$).

[d] $S = [\Sigma w(F_o^2 - F_c^2)^2/(n-p)]^{1/2}$ (n = number of data; p = number of parameters varied; $w = [\sigma^2(F_o^2) + (0.0434P)^2 + 0.8092P]^{-1}$ where $P = [\text{Max}(F_o^2, 0) + 2F_c^2]/3$).

[e] $R_1 = \Sigma||F_o| - |F_c||/\Sigma|F_o|$; $wR_2 = [\Sigma w(F_o^2 - F_c^2)^2/\Sigma w(F_o^4)]^{1/2}$.

References

[1] (a) W.J. Evans, Polyhedron 6 (1987) 803. (b) C.J. Schaverien, Adv. Organomet. Chem. 36 (1994) 283. (c) F.T. Edelmann, Comprehensive Organometallic Chemistry II, vol. 4, Pergamon, Oxford, 1995, Ch. 2.

[2] F.T. Edelmann, Angew. Chem. Int. Ed. Engl. 34 (1995) 2466.

[3] G.B. Deacon, E.E. Delbridge, B.W. Skelton, A.H. White, Eur. J. Inorg. Chem. (1999) 751, and references therein.

[4] (a) J. Takats, X.W. Zhang, V.W. Day, T.A. Eberspacher, Organometallics 12 (1993) 4286. (b) G.H. Maunder, A. Sella, D.A. Tocher, J. Chem. Soc. Chem. Commun. (1994) 885. (c) A. Domingos, J. Marçalo, N. Marques, A. P. Dematos, A. Galvao, P. C. Isolani, G. Vincenti, K. Zinner, Polyhedron 14 (1995) 3067.

[5] (a) Z. Hou, Y. Zhang, T. Yoshimura, Y. Wakatsuki, Organometallics 16 (1997) 2963. (b) Z. Hou, J. Alloys Comp., in press.

[6] (a) L. Hasinoff, J. Takats, X. W. Zhang, A. H. Bond, R. D. Rogers, J. Am. Chem. Soc. 116 (1994) 8833. (b) J. Takats, J. Alloys Comp. 249 (1997) 52. (c) X. W. Zhang, Ph.D. Thesis, University of Alberta, 1995.

[7] G.M. Ferrence, R. McDonald, J. Takats, Angew. Chem. Int. Ed. Engl. 38 (1999) 2233.

[8] (a) M.F. Lappert, P.I.W. Yarrow, J.L. Atwood, R. Shakir, J. Chem. Soc. Chem. Commun. (1980) 987. (b) J.R. van den Hende, P.B. Hitchcock, M.F. Lappert, T.A. Nile, J. Organomet. Chem. 472 (1994) 75.

[9] X.W. Zhang, R. McDonald, J. Takats, New J. Chem. 19 (1995) 573.

[10] Y.M. Sun, R. McDonald, J. Takats, V.W. Day, T.A. Eberspacher, Inorg. Chem. 33 (1994) 4433.

[11] A.C. Hillier, S.Y. Liu, A. Sella, M.R.J. Elsegood, J. Alloys Comp., in press.

[12] J.L. Kisko, T. Hascall, C. Kimblin, G. Parkin, J. Chem. Soc. Dalton Trans. (1999) 1929.

[13] C.M. Dowling, D. Leslie, M.H. Chisholm, G. Parkin, Main Group Chem. 1 (1995) 29.

[14] J.J. Songchun, W. Chen, J. Organomet. Chem. 412 (1991) 71.

[15] T.D. Tilley, R.A. Andersen, B. Spencer, A. Zalkin, Inorg. Chem. 21 (1982) 2647.

[16] T.D. Tilley, R.A. Andersen, B. Spencer, H. Ruben, A. Zalkin, D.H. Tempelton, Inorg. Chem. 19 (1980) 2999.

[17] P.B. Hitchcock, J.A.K. Howard, M.F. Lappert, S. Prashar, J. Organomet. Chem. 437 (1992) 177.

[18] C.J. Burns, Ph.D. Thesis, University of California, Berkeley, 1987.

[19] R.D. Shannon, Acta Crystallogr. Sect. A 32 (1976) 751.

[20] G.M. Ferrence, X.W. Zhang, M. Morissette, R. McDonald, J. Takats, unpublished results.

[21] (a) J.L. Atwood, K.D. Smith, J. Am. Chem. Soc. 95 (1973) 1488. (b) S.H. Eggers, H. Schultze, J. Kopf, R.D. Fischer, Angew. Chem. Int. Ed. Engl. 25 (1986) 656. (c) C. Apostolidis, G.B. Deacon, E. Dornberger, F.T. Edelman, B. Kanellakopulos, P. MacKinnon, D. Stalke, Chem. Commun. (Cambridge) (1997) 1047.

[22] H. Schumann, J.A. Meese-Marktscheffel, L. Esser, Chem. Rev. 95 (1995) 865.

[23] I. Lopes, G.Y. Lin, A. Domingos, R. McDonald, N. Marques, J. Takats, J. Am. Chem. Soc. 121 (1999) 8110.

[24] G.Y. Yin, V. Te, R. McDonald, J. Takats, unpublished results.

[25] G.B. Deacon, E.E. Debbridge, C.M. Forsyth, Angew. Chem. Int. Ed. Engl. 38 (1999) 1766.

[26] J.R. Perera, M.J. Heeg, H.B. Schlegel, C.H. Winter, J. Am. Chem. Soc. 121 (1999) 4536.

[27] M.C. Cassani, D.J. Duncalf, M.F. Lappert, J. Am. Chem. Soc. 120 (1998) 12958.

[28] Programs for diffractometer operation, data collection, data reduction and absorption correction were those supplied by Brüker.

[29] G.M. Sheldrick, Acta Crystallogr. Sect. A 46 (1990) 467.

[30] G.M. Sheldrick, SHELXL-93. Program for crystal structure determination, University of Göttingen, Germany, 1993.